

Evolution of the crystallite size of Erbium Tetrapolyphosphate with heat treatment or oxidation

Evolution de la taille des cristallites du Tertapolyphosphate d'Erbium avec le traitement thermique ou l'oxydation

Bouazza Tbib¹, Mohammed Eddya¹, Khalil El-Hami¹

¹ Laboratory of Nanosciences and Modeling, University of Hassan 1st, Faculty of Khouribga, Morocco, bouazza.tbib@gmail.com, eddya.mohammed1@gmail.com, khalil.elhami@uhp.ac.ma

ABSTRACT. Our study focuses on the influence of the oxidation temperature on the crystallite size, oxidation kinetics and mechanisms associated with the oxidation of Erbium Tetrapolyphosphate (TPE). We compared the evolution of the crystallographic morphology of the TPE powder subjected to a heat treatment at high temperature between 200 ° C and 1100 ° C. The evolution of the crystallite size of the powder was demonstrated by X-rays diffraction. The structural units of phosphate-based glass were assessed from Raman spectra as TPE; the results show the decomposition of powder in the temperature range of 850° -1100°C. Er³⁺ absorption spectra were measured in the range of 400-800 nm. Optical bandgap (E_g) were determined using Tauc's relationship for direct transitions.

RÉSUMÉ. Notre étude se concentre sur l'influence de la température d'oxydation sur la taille des cristallites, la cinétique d'oxydation et les mécanismes associés à l'oxydation de l'Erbium Tetrapolyphosphate (TPE). Nous avons comparé l'évolution de la morphologie cristallographique de la poudre du TPE soumis à un traitement thermique variant entre 200°C et 1100°C. L'évolution de la taille des cristallites de la poudre a été déterminée par la diffraction des rayons X. Les unités structurales du verre à base de phosphate sous forme de TPE ont été évaluées à partir des spectres Raman. Les résultats montrent la décomposition de la poudre dans la plage de température de 850-1100°C. Les spectres d'absorptions de TPE ont été mesurés dans la plage de 400 à 800 nm. Les bandgap optique (E_g) ont été déterminées en utilisant la relation de Tauc pour les transitions directes.

KEYWORDS. Grain size, Polyphosphate, X-ray diffraction, Raman spectroscopy, optical bandgap.

MOTS-CLÉS. Taille des grains, Polyphosphate, diffraction des rayons X, Spectroscopie Raman, Bandgap optique.

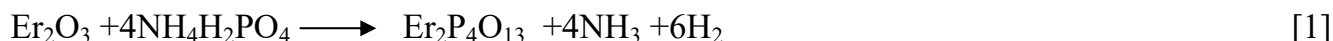
1. Introduction

All material such is hold an amount of Erbium element, it used in surface treatment [ZHE 13], thus Erbium can be used in the emission of red and green light of the blow is applied a pressure stress the emission increases, the future prospects for applications of Er³⁺ based PL materials in various fields, such as high power lasers and (bio) medical imaging [HON 17]. Moreover, up-conversion is the reverse process, where two low frequency photons are converted to a single high-frequency photon. Therefore, down- and up-conversion correspond to a frequency conversion of the photons through a nonlinear interaction. The up/down term correspond to the "direction" of the frequency change [WAN 18]. Inorganic pyrophosphates can be used in light-emitting diodes (LEDs) converted to phosphorus. The pyrophosphates are the host networks suitable for activators because of their high uptake in the UV region, excellent chemical and thermal stability [HAI 14 , FAN 17]. The effect of the element erbium, used as additive by various methods to prepare the electrode be positive, on the high-temperature performances of batteries Ni-MH. It found that the capacity of acceptance of load of the spherical electrode Ni(OH)₂ with the element erbium as additive is improved. The capacities of discharge of Ni(OH)₂ dressed in 1% (atomic fraction) Er(OH)₃ and added mechanically to 1% (atomic fraction) Er₂O₃ in 1 °C are respectively 12,6 % and 11,7 % superior to those of the samples without erbium in 70 °C. The emission spectra ex- cited at 779 nm comprises of 518 nm, 550 nm and 649 nm of transition ⁴F_{9/2}, ⁴S_{3/2} and ²H_{11/2} excited states to ⁴I_{15/2} ground state and the physical and optical properties of ultra-phosphate glass influenced by erbium, it can give important information for a broader development of functional glass [ALI 18]. In this study, we have followed, in particular, the

evolution of the grain size of erbium pyrophosphates subjected to a heat treatment between 200 and 1100 °C, for varying periods. The variation of the crystallite size of erbium pyrophosphates has been demonstrated by X-ray diffraction.

2. Experimental process: Synthesis of TPE by solid state method

For the synthesis of TPE by solid way, the reactive of departure, purity of Erbium Oxide Nano powder Er_2O_3 : 99.9 %, Color pink (Aldrich, 99.997 %) and Ammonium of hydrogen phosphates (ADP) $\text{NH}_4\text{H}_2\text{PO}_4$ appearances white crystals (Fluka, 99 %). The mixture was then treated thermally in 200°C to eliminate water molecules absorbed during 24 hours then in 450°C counterparts 24 hour to decompose the dihydrogen ammonium phosphorus $(\text{NH}_4)_2\text{HPO}_4$ then between 600 and 1000°C necessary for the obtaining of the phase $\text{Er}_2\text{P}_4\text{O}_{13}$, the precursors so to formed were then crushed between every treatment, the chemical reaction is:



The table 1 show the masses molars, and masses synthesis of $\text{Er}_2\text{P}_4\text{O}_{13}$ (TPE), and the figure 1 show the photograph of TPE between 25 °C and 1000 °C.

compounds	Er_2O_3	$\text{NH}_4\text{H}_2\text{PO}_4$	$\text{Er}_2\text{P}_4\text{O}_{13}$ (TPE)
masses molars (g/mol)	382.5162	115.0257	666.4052
masses (g)	5.7399	6.9042	10g
Color	pink	white	pink

Table 1. Precursors and TPE product masses molars, and masses

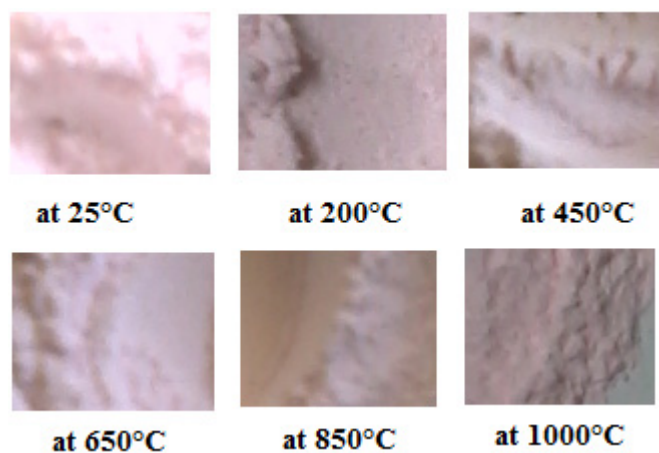


Figure 1. Photographs of TPE at different temperatures

3. Results and Discussion

3.1. X-ray diffraction analysis

3.1.1. Structural parameters

All the handled samples were analyzed by diffraction X. This technique allowed to define the size of the crystallites of the Tetrapolyphosphates $\text{Er}_2\text{P}_4\text{O}_{13}$ before and after treatment of annealing or oxidation. For sizes of grains lower than 100 nm, we observe a very important extension of the lines of diffraction. Figure 2 shows the X-ray diffraction patterns of the powder of Erbium polyphosphate $\text{Er}_2\text{P}_4\text{O}_{13}$ taken in a 2θ range from 12 to 60° . All the reflections peaks were indexed in the monoclinic system Space group P/2m. the parameters generated by Fullprof program as shown in table 2. The effect of temperature on the Tetrapolyphosphates $\text{Er}_2\text{P}_4\text{O}_{13}$, such as the grains size, displacement of position and intensity, have been studied in the temperature range 200°C to 1100°C .

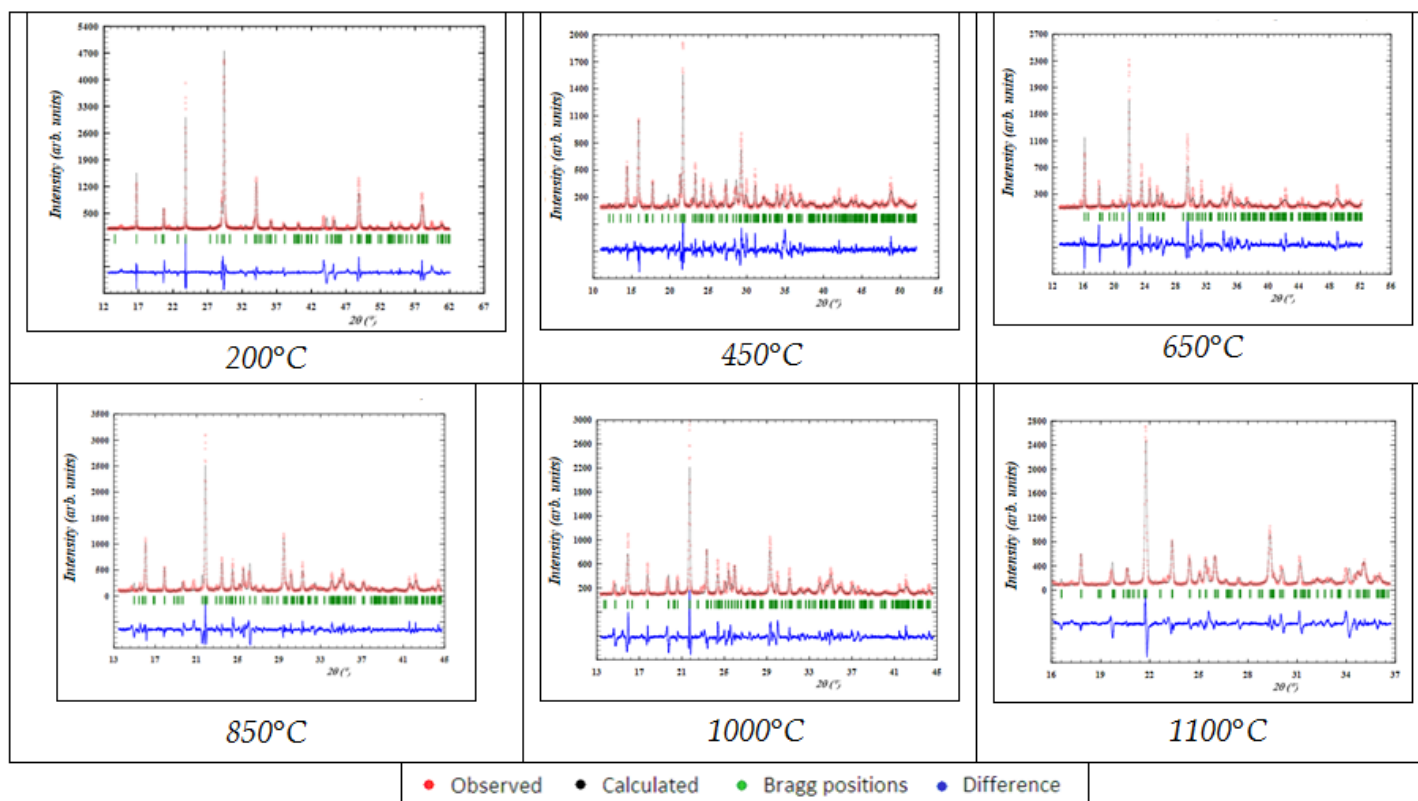


Figure 2. TPE X-ray spectrums of various temperature 200 to 1100 °C

Temperature °C	a[Å]	b[Å]	c[Å]	Beta[°]	V[Å ³]	Space group	Crystal System
200°C	13.0410	9.1173	2.6336	90.000	313.1340	P m m m	Orthorhombic
450°C	12.3908	8.5897	8.3871	97.040	885.9364	P 2/m	Monoclinic
650°C	11.0013	10.6955	4.9126	93.541	576.9401	P 2/m	Monoclinic
850°C	11.7590	5.9257	11.4520	102.369	779.4608	P 2/m	Monoclinic
1000°C	15.2633	3.8090	13.1826	100.943	752.4796	P 2/m	Monoclinic
1100°C	9.5208	9.9620	9.0964	109.945	811.0113	P 2/m	Monoclinic

Table 2. Cell parameters extracted from full pattern refinements of various temperature of TPE

The figure 3 shows the variation of the parameters of cell of TPE, according to the temperature. This regular evolution shows that we have a solid solution. We observe an increase of the parameter (c) and a decrease of the parameters a and b. These variations can give some explanation within the framework of the crystalline structure of these poly phosphates, formed by a three-dimensional chain (sequence of movements) of groupings P_2O_7 and pyramids on squared base ErO_5 . The decrease of parameterizes b and c can be connected the grain size of tetrapolyphosphates $Er_2P_4O_{13}$. The increase or the decrease of the parameters of the cell can be bound to the elasticity of the network trained by groupings bound only by summits.

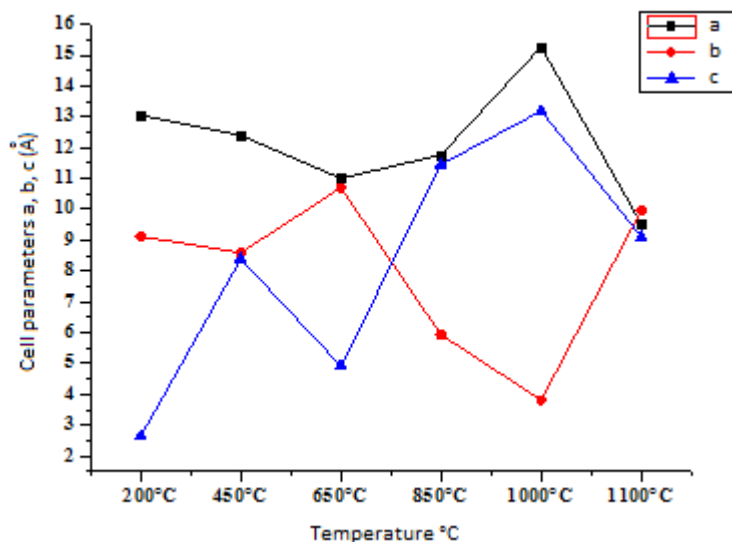


Figure 3. Variation of the TPE cell parameters function temperature

3.1.2. Crystallite size

To make the distinction between the effect of the heat treatment for high temperature, and that of the oxidation, we followed, by analysis in diffraction RX, the evolution of the thickness of grains the solid solution tetrapolyphosphates $Er_2P_4O_{13}$. Crystal size or average diameter of the crystallites could be calculated using Debye-Scherrer equation [STA 6]:

$$L = (D * \lambda) / (\beta * \cos(\theta)) \quad [2]$$

θ is the Bragg angle, λ is the wavelength of X-ray used (CuK radiation) = 1,54056 Å, L is the crystal size, and D is the shape factor which is approximately unity. β is the line broadening at half the maximum intensity (FWHM).

The obtained values of crystallite size and strain at different annealing temperatures are illustrated in Figure 4. The temperature has a significant impact on the material. We noticed a decrease of crystallites, the values of crystallites are determined from the width halfway up (FWHM) of the intense peak by using the relation of Scherrer. We observed that the size of the crystallites of the TPE decreases only very slightly until 850°C then she resumed an increase accelerated until 1100°C. For the size of the crystallites of TPE in 200°C (59.84 nm), the size of the crystallites of TPE in 450°C (56.51 nm), the size of the crystallites of TPE in 650°C (43.56 nm), the size of the crystallites of TPE in 850°C (32.36 nm), the size of the crystallites of TPE in 1000°C (39.26 nm) and the size of the crystallites of TPE as shown in the table 3. On the other hand, the size of the crystallites of TPE believes abruptly from 850°C. This strong increase is going to lead a significant decrease of the density of materials. The change of the size of crystallites can understand if we take into account the strong thermal dilation of materials.

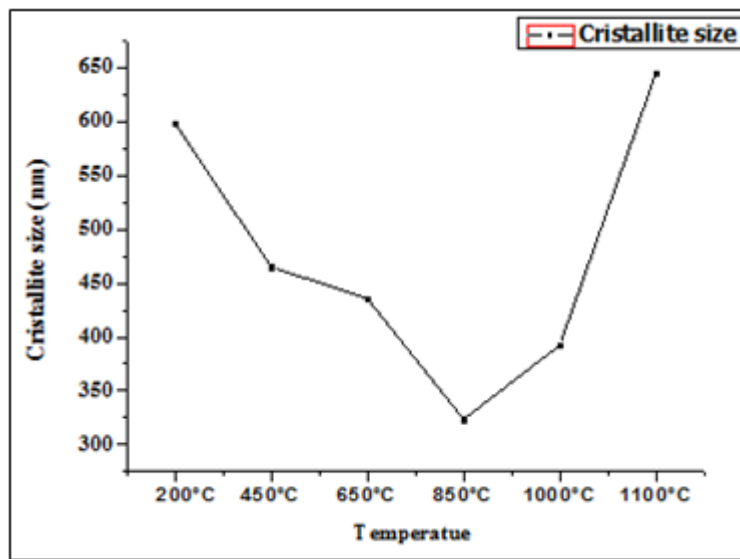


Figure 4. Variation of crystallite size for TPE as a function of at a high temperature

Temperature °C	Crystallite size (A°)
200°C	598,406671
450°C	465,173137
650°C	435,619324
850°C	323,665361
1000°C	392,644911
1100°C	645,841638

Table 3. Crystallite size of TPE in different temperatures

3.1.3. Microstrain

The temperature is an important effect on the microscopic mechanism the constraint, which deformed the material, the microstructure represented as an energy stored in the material, when the temperature increases the easier and plastic deformation furthermore we deduced in constant temperature, when the speed of deformation increases, the constraint must be higher to deform, this thermal ageing is going to apply a corrosion to the environment we also said the defects move with the rise of the temperature, moreover, the dislocations are trapped in the directions dense crystallographic this movement connected to the intra-atomic and inter atomic interactions so with the environment This process of growth is accelerated in $T = 1100^{\circ}\text{C}$, with the size of with the size of grains approaches or quickly penetrates into the region of the micrometer. The figure 5 and figure 6 represents respectively the variation of microstrain function of temperature and 2θ . These observations indicate that the temperature is a parameter effective thermodynamics, which controls the process of crystallization, because the growth of grains comes along typically with atomic rearrangements at long distance, she would be kinetically hindered [ZHA 8].

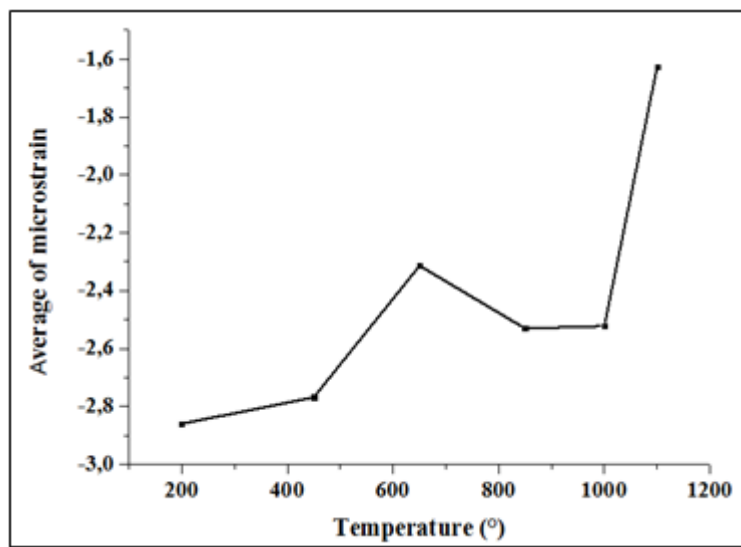


Figure 5. Variation of average microstrain for TPE as a function of at a high temperature

The XRD method is used to analyze structure parameters such as microstrain, crystallite size and dislocation density. The knowledge of such parameters especially for new materials is important prior to their technical applications. XRD analysis is also employed to identify details about phase compositions, crystal preferred orientations and crystal defect concentrations. Stokes deconvolution method combined with the Warren Averbach analysis, which are based on the XRD broadened line analysis are the most rigorous and unbiased approach to obtain the true specimen broadened profile and related microstructural parameter. The approximation method was also useful in determining microscopic parameters of crystallite size and microstrain. When a polycrystalline material is deformed elastically such that the strain is uniform over relatively large distances the lattice plane spacings in the crystal change from their stress free values to new values corresponding to the stress and appropriate elastic constants. These are usually referred as macrostrains, where plastic deformation occurs the local distortion of lattice planes gives rise to non-uniform variations in the inter plan spacing.

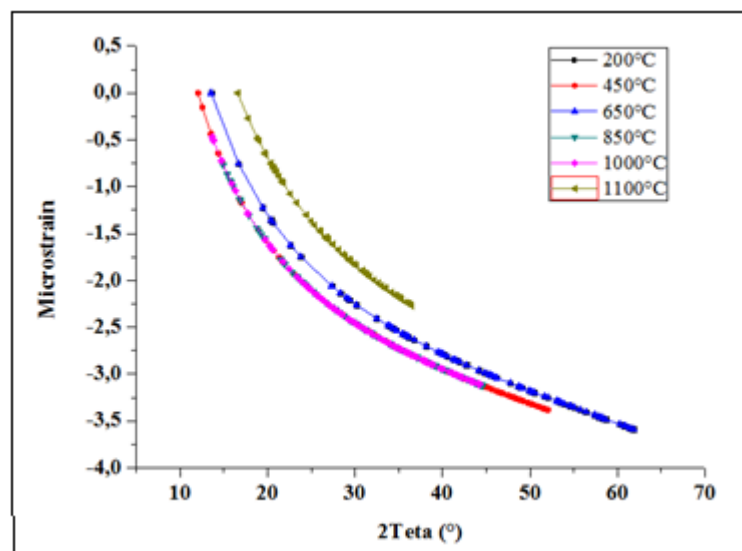


Figure 6. The variation of microstructures according to 2θ of TPE in various temperatures

3.2. Raman spectroscopy

The figure 7 presents the Raman's spectrum collected on the powder of TPE observing few peaks. The recording specter from 0 to 3500 cm^{-1} also we observe a part enlarged by specter of Raman for the powder of TPE in 200°C , the specter of Raman was applied to study the vibrations of the network of

TPE in 200°C. There is a more intense peak in 880 cm^{-1} with several signals low(weak) intensity between 250 and 250 cm^{-1} , the intense peak corresponds to the vibration of $(\text{PO}_4)^{3-}$ [SAS 15, MOG 10] and towards 375 cm^{-1} we find the vibration of the band (O - P - O) [MOU 98, ARD 07], and between 625 cm^{-1} - 800 cm^{-1} the symmetric vibration of the band (P-O-P) [SCH 04]. In addition, we observed that the intense peak shape is broad corresponding to the amorphous powder at 200°C.

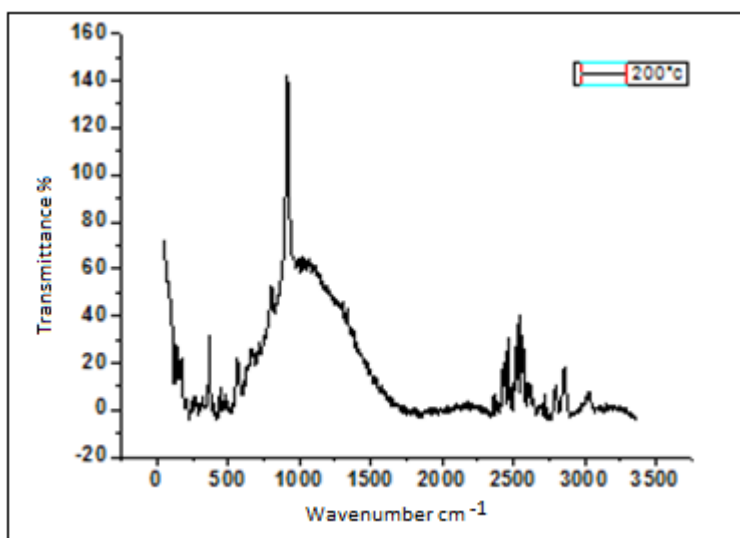


Figure 7. Raman spectra of TPE at temperature 200°C

In figure 8, we observe the disappearance of intense peaks between 250 cm^{-1} and 3500 cm^{-1} that, in stead off, two bands appear respectively in 750 cm^{-1} -1500 cm^{-1} and 1750 cm^{-1} -2500 cm^{-1} . We suggest, those of decomposition of the precursors of more disappearance of volatile elements at 450°C. At this temperature, the oxidation is controlled by a surface reaction governed by the preferential diffusion mechanism around grain boundaries. Oxidation occurs more rapidly at the level of intergranular oxidation. In addition, the presence of temperature promotes the growth of TPE formation.

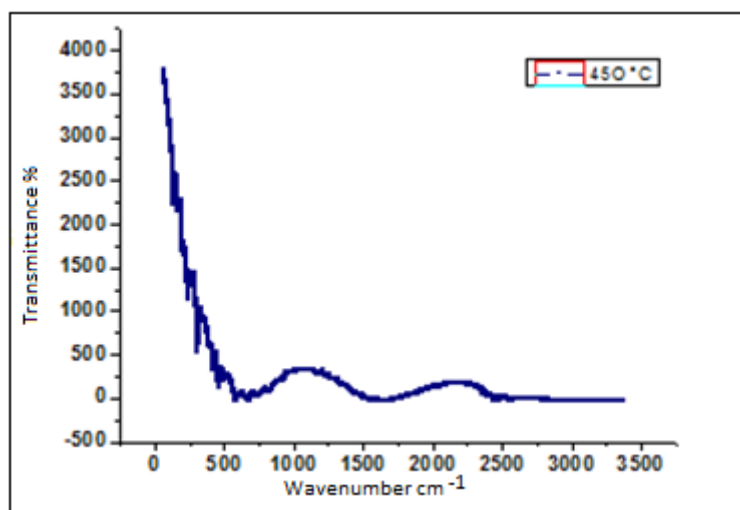


Figure 8. Raman spectra of $\text{Er}_2\text{P}_4\text{O}_{13}$ at temperature 450°C

At 650 °C, the spectrum returns to the initial shape of 200 °C but with the appearance of a spectrum around 3250 cm^{-1} , these peaks meant the beginning of the formation of the TPE phase as you see in the figure 9.

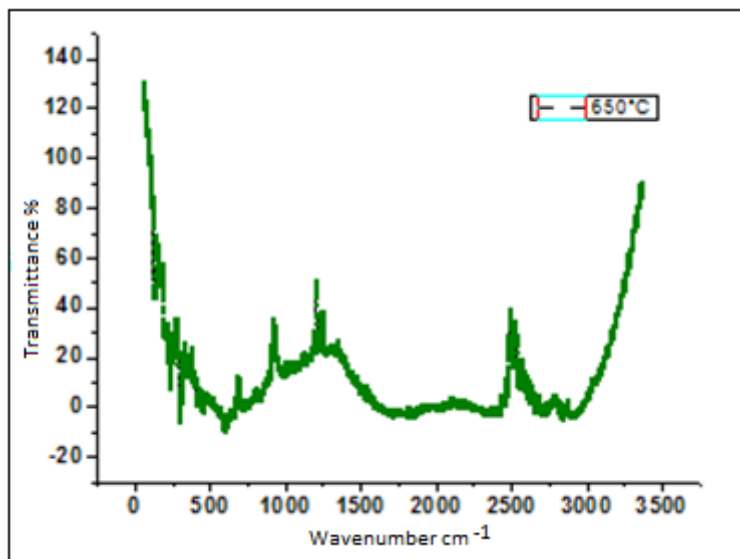


Figure 9. Raman spectra of TPE at temperature 650 °C

The powder is treated at high temperature between 850 °C and 1100 °C and was characterized by Raman spectroscopy as shown in Figures (10-11-12). We notice that the spectrum is changed totally and remained at the same shape, same position for the intense peak up to the temperature 1100°C. Moreover, the intensity is changed according to temperature. The peak of strong intensity appear at 2500cm^{-1} and other peaks of average intensities appear between 250 cm^{-1} and 1500 cm^{-1} . These peaks attributed to the vibration mode of deformation of phosphate tetrahedra (P-O) and deformations to long distance of the crystal lattice (P-O). In figures (10-11-12, intense and strong peaks, as well as a doublet of low intensity, respectively corresponding to symmetric and asymmetric stretching vibration modes of the isolated phosphates (VP- O). The difference between the spectra recorded at 200°C and the temperature of the TPE phase formation, namely the very low peak intensities at low angles and the peak broadening during heat treatment, confirm a structural change of TPE for the stress reached. All TPE Raman spectrum are grouped in figure 13.

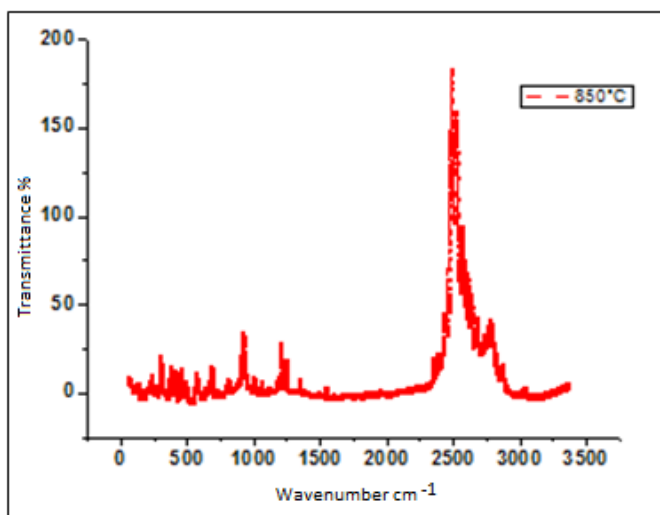


Figure 10. Raman spectra of TPE at 850°C

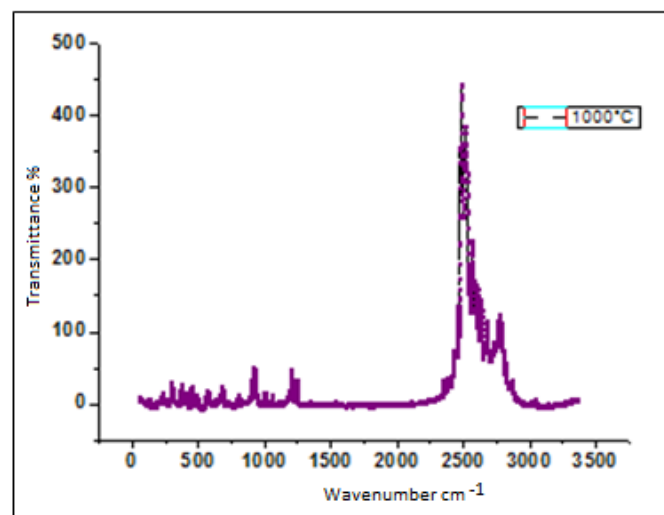


Figure 11. Raman spectra of TPE at 1000°C

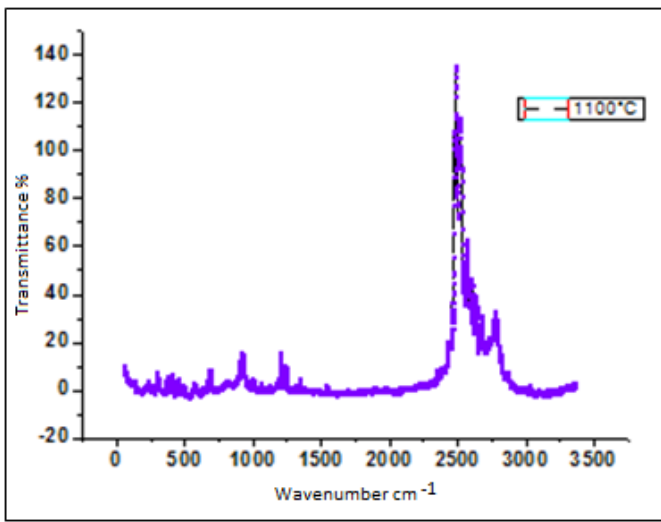


Figure 12. Raman spectra of TPE at 1100°C

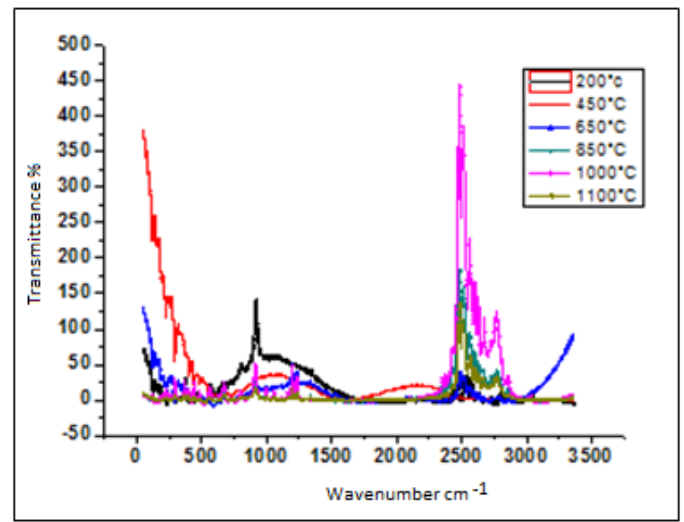


Figure 13. Raman spectra of TPE between 200 and 1100°C

In table 4, the position of the intense peak is considered as a function of the treatment temperature. We follow the dependence of the movement of the peaks with high frequencies when the temperature increases. Figure 14 shows that, peak intensity increases up to 800°C which attests the distortion of chains and a stress increase in the material at high temperature. The material is partially disordered as confirmed by the broadening of peaks in the Raman spectrum. Above the temperature of 800°C, a linear curve is observed and continuous during high temperature confirming the presence of the final structure of TPE.

Temperature (°C)	Position of intense peak cm ⁻¹
200	880
450	1000
650	1250
850	2500
1000	2500
1100	2500

Table 4. The position of intense peak and temperature of treatment

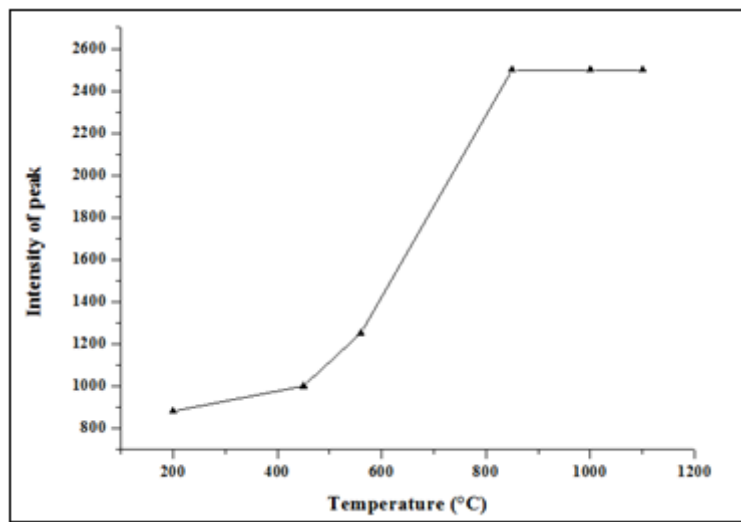


Figure 14. Intensity variation of TPE Raman spectrum following heat treatment

3.2. X-Ray Fluorescence (XRF)

Characterization and analysis were also performed on every sample of TPE by using the X-ray fluorescence (XRF) which will be analyzed the content of phosphorus and of erbium. Results can be seen in the table 5 below, which consists essentially of phosphorus and of erbium. The effect of the temperature on the TPE cannot reduce the content of phosphorus and of erbium in the material TPE. We find a small variation as shown in figure 15. The concentrations of phosphorus and erbium show that the content averages (Cm) in phosphorus in the TPE is about 11.44 % and that erbium found in the TPE is about 109.42 %. We notice the this kind of characterization provide information on both composition and identification the purity of material TPE for reability.

Temperature (°C)	Compound and Concentration (%)	
	P	Er
200	13,066	105,947
450	10,943	108,883
650	11,175	107,061
850	11,524	11,524
1000	11,305	110,06
1100	10,676	115,308

Table 5. Phosphorus and erbium concentration measurement in TPE

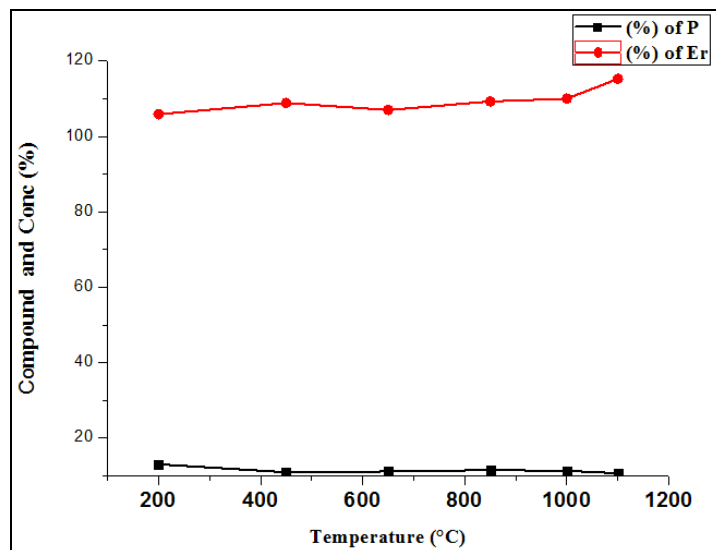


Figure 15. Variation of phosphorus and Erbium concentrations following the heat treatment.

4. Conclusion

We prepared the Erbium Tetrapolyphosphate (TPE) new material with chemical formula $\text{Er}_2\text{P}_4\text{O}_{13}$ at various temperatures and determined their unit cell parameters. When the temperature of a solid change, we observe generally a variation of its length (surface and volume also). Increasing temperature usually produces a dilation (increase of the dimensions), whereas a decrease of temperature pulls a contraction (decrease of the dimensions). The results of decreased quantum seclusions when 2θ increase and the grain size dependance with temperature may find application in energy field.

Bibliography

- [ZHE 13] K. Zheng, Z. Liu, Ye Liu, W. Song, and Weiping .Influence of core size on the upconversion luminescence properties of spherical $\text{Gd}_2\text{O}_3:\text{Yb}^{3+}/\text{Er}^{3+}/\text{SiO}_2$ particles with core-shell structures Qin,*J. Appl. Phys*,114, 183109 (2013)
- [HON 17] F. Hong Binbin, YueBinbin YueZ. X. ChengZ. X. Cheng Ho-Kwang Mao. Pressure-enhanced light emission and its structural origin in Er: GdVO_4 , *Applied Physics Letters* 110(2):021903, (2017)
- [WAN 18] De-Yin Wang, Ma. Pengchen, Jiachi Zhang, and Yuhua Wang.Efficient down- and up-conversion luminescence in Er^{3+} - Yb^{3+} codoped $\text{Y}_7\text{O}_6\text{F}_9$ for photovoltaics. *ACS Appl. Energy Mater*, (2018)
- [HAI 14] JI, Haipeng, HUANG, Zhaohui, XIA, Zhiguo, et al. New yellow-emitting whitlockite-type structure $\text{Sr}_{1.75}\text{Ca}_{1.25}(\text{PO}_4)_2$: Eu^{2+} phosphor for near-UV pumped white light-emitting devices. *Inorganic chemistry*, vol. 53, no 10, p. 5129-5135 (2014).
- [FAN 17] Y.T. Fan, M. Tang, Z.X. Qiu, J.L. Zhang, L.P. Yu, C.Z. Li, S.X. Lian, W.L. Zhou, *J. Solid State Chem.* 246 194e198 (2017).
- [ALI 18] M. Aliyu, R. Hussin Karim Deraman,N. E.Ahmad,Amina M. Danmadamiy and Y.A. Yamusa,'Physical and optical properties of calcium sulfate ultra-phosphate glass doped Er_2O_3 ',*International Journal of Modern Physics B*,Vol. 32 1850084(2018).
- [STA 6] D. A. Stankovich, G. H. B. Dikin, K. M. Dommert, E. J. Kohlhaas, E. A. Zimney, R. D. Stach, S. B. T. Piner Nguyen, and R. S. Ruoff, Graphene-based composite materials, *Nature* 442, 282-286, (2006).
- [ZHA 8] Y. Zhao and J. Zhang, ' Microstrain and grain-size analysis from diffraction peak width and graphical derivation of highpressure thermomechanics', *J. Appl. Cryst.* 41, 1095–1108 (2008).
- [SAS 15] S. Sastry, S. Rao, B. Rupa Venkateswara. Spectroscopic characterization of manganese-doped alkaline earth lead zinc phosphate glasses. *Bulletin of Materials Science*, vol. 38, no 2, p. 475-482 (2015).

- [MOG 10] Mogus-Milankovic, A. Pavic, L. Reis, T. Signo, et al. Structural and electrical properties of Li₂O–ZnO–P₂O₅ glasses. *Journal of non-crystalline solids*, vol. 356, no 11-17, p. 715-719 (2010).
- [MOU 98] Y. M. Moustafa, K. El-Egli, Infrared spectra of sodium phosphate glasses. *Journal of non-crystalline solids*, vol. 240, no 1-3, p. 144-153 (1998).
- [ARD 07] I. Ardelean, D. RUSU, C. ANDRONACHE, et al. Raman study of xMeO·(100– x)[P₂O₅· Li₂O](MeO ⇒ Fe₂O₃ or V₂O₅) glass systems. *Materials Letters*, vol. 61, no 14-15, p. 3301-3304 (2007).
- [SCH 04] J. Schwarz, H. L. TICHÁ, R. Tichý a, J. Mertens, Optoelectron. *Adv. Mater*, vol. 6, no 3, p. 737-746 (2004).